Chemoselective and Enantioselective Fluorescent Recognition of Prolinol

Yixuan Jiang[†a], Jun Tian[†a], Hongyu Guo[a], Yan Gong[a], Shanshan Yu*[a], Xiaoqi Yu[a], Lin Pu*[b]

[a]*Key Laboratory of Green Chemistry and Technology, Ministry of Education, College of Chemistry, Sichuan University, Chengdu, China 610064.*

[b]*Department of Chemistry, University of Virginia, Charlottesville, Virginia 22904, USA*

**Corresponding author e-mail: lp6n@virginia.edu yushanshan@scu.edu.cn*

†Y. J. and J. T. contributed equally to this work.

Abstract. A highly chemoselective and enantioselective fluorescent probe has been discovered for the recognition of prolinol among various primary and secondary amine-based amino alcohols. The mechanistic studies including 1D and 2D $^{1}H/^{13}C$ NMR and mass spectroscopic analyses and DFT calculations have shown that the aldehyde group of the probe can react with prolinol to generate a bicyclic oxazolidine unit which through a possible intramolecular hydrogen bond interaction to give highly selective fluorescence enhancement.

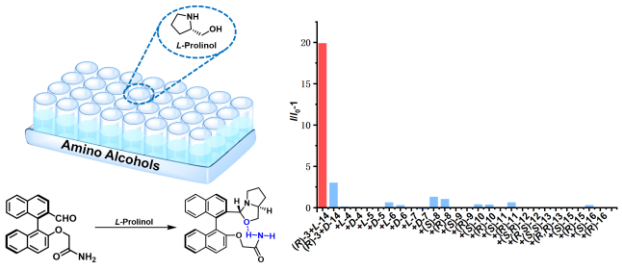

Introduction

Enantioselective fluorescent recognition of chiral organic molecules can potentially provide a fast-analytical tool for chiral assay.[1] Chiral amino alcohols are very useful in the asymmetric synthesis of diverse organic compounds.[2] Fluorescent probes that can distinguish the enantiomers of chiral amino alcohols have been obtained which can be used to determine the enantiomeric composition of a variety of substrates.[3] While it is important to develop fluorescent probes that are generally useful in the recognition of certain classes of compounds, a fluorescent probe that shows chemoselective as well as enantioselective responses toward a specific substrate is also of significant interest. For example, such a probe could be used to detect a specific enantiomeric molecule produced in reactions or catalyst screening experiments or present in analytical samples.

Previously, we demonstrated that the 1,1'-binaphthyl-based compound (*S*)-**1** shows fluorescence enhancement in the presence of prolinol in the *absence* of a metal ion like Zn^{2+}.[4,5] However, no enantioselectivity in the fluorescence response was observed.[4] In order to improve the selectivity of (*S*)-**1**, we have explored a

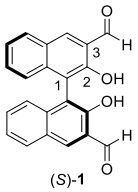

(*S*)-**1**

strategy to modify the structure of the probe by moving the amine-binding aldehyde group from the 3-position to the 2-position to be closer to the chiral cavity of the 1,1'-binaphthyl core. The resulting compounds have shown unique fluorescence responses in molecular recognition.[6,7] Herein, we report a new discovery that a 1,1'-binaphthyl compound containing a 2-aldehyde group and an acetamide unit exhibits chemoselective as well as enantioselective fluorescent response toward prolinol. Such a selective fluorescent probe is potentially useful since prolinol is a chiral amino alcohol of broad applications in synthesis and drug discovery[8] and it has also been found as a metabolite in cancer metabolism.[9] Our study on the origin of the selective fluorescence response is also presented.

Results and Discussion

We incorporated an acetamide group that is capable of hydrogen bond donating as well as accepting into a 2-formy-1,1'-binaphthyl structure as shown in Scheme 1. Compound (*R*)-**2** was prepared according to our previously reported method.[7] Treatment of (*R*)-**2** with 2-bromoacetamide in the presence of K_2CO_3 gave (*R*)-**3** in 83% yield. The two inequivalent amide protons were observed at δ 5.37 (br) and 5.00 (br) in the ^{1}H NMR spectrum of (*R*)-**3**. The two diastereotopic proton signals of H_x and $H_{x'}$ were observed at δ 4.49 (d, J = 15.3 Hz) and 4.45 (d, J = 15.2 Hz). The UV-vis absorption and fluorescence spectra of (*R*)-**3** in *i*-PrOH were obtained. As shown in Figure 1, (*R*)-**3** gives absorptions at λ(ε) = 229 (8.90×10^4), 251 (4.79×10^4), 286 (1.57×10^4) and 333 (4.75×10^3) nm [ε in L/(mol·cm)]. When it was excited at 285 nm, there was a weak emission at 360 nm.

Scheme 1. Synthesis of compound (*R*)-**3**.

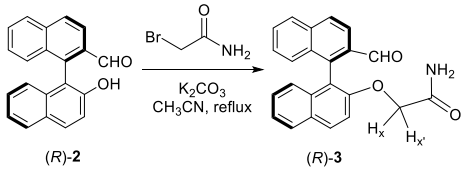

(*R*)-**2** (*R*)-**3**

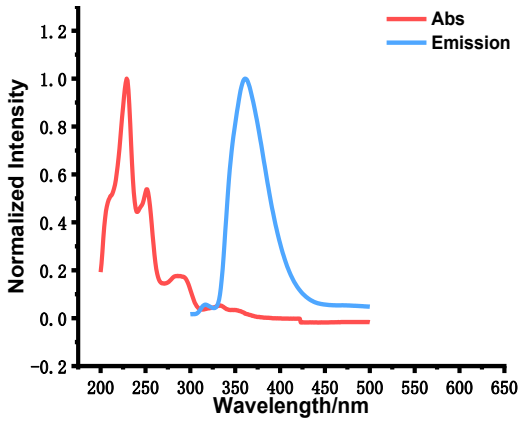

Figure 1. Normalized UV-vis and fluorescence spectra of (*R*)-**3** (2.0×10^{-5} M in *i*-PrOH) (λ_{exc} = 285 nm).

We studied the fluorescence response of (*R*)-**3** toward a variety of chiral amino alcohols as listed in Figure 2. In these experiments, a solution of (*R*)-**3** (2.0×10^{-3} M, 25 μL) in *i*-PrOH was mixed with each enantiomer of an amino alcohol (6.0 equiv) in *i*-PrOH at 30.0 °C for 3.0 h, then diluted with *i*-PrOH to a final concentration of (*R*)-**3** at 2.0×10^{-5} M. As shown in Figure 3, among the primary amine-based substrates **4** - **13** and the secondary amine-based substrates **14** - **16**, only *L*-prolinol (*L*-**14**) greatly enhanced the fluorescence of (*R*)-**3** at λ = 360 nm with a fluorescence enhancement factor (I/I_0-1) of 20.0. The opposite enantiomer *D*-prolinol as well as other amino alcohols generated little fluorescence response with the probe. Therefore, (*R*)-**3** is both highly chemoselective and enantioselective in the fluorescent recognition of prolinol. (All the fluorescence spectra are in Figure S1 in SI). In other solvents such as acetonitrile, 1,4-dioxane and ethanol, (*R*)-**3** also showed enantioselective fluorescent enhancement with *L*-prolinol (see Figure S2 in SI).

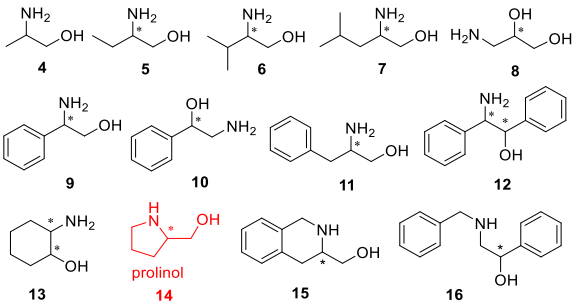

Figure 2. Chiral amino alcohols used to interact with (*R*)-**3**.

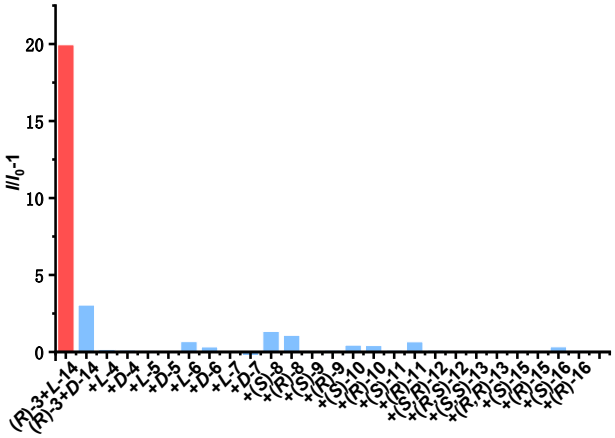

Figure 3. Fluorescent responses at λ = 360 nm, I_{360}/I_0-1, for the interaction of (*R*)-**3** (2.0×10^{-5} M) with 13 pairs of amino alcohol enantiomers (6 equiv) (Solvent: *i*-PrOH. λ_{exc} = 285 nm, slits = 5/5 nm. I_0: Fluorescence intensity of (*R*)-**3** at 360 nm in the absence of amino alcohols).

The fluorescence responses of (*R*)-**3** versus the concentration of *L*- and *D*-prolinol was investigated. The reaction time between (*R*)-**3** and prolinol in *i*-PrOH before dilution was chosen to be 3.0 h on the basis of a reaction time study shown in Figure S3 of SI. The fluorescence intensity of (*R*)-**3** at λ = 360 nm greatly increased with the addition of 0.5 equiv to 6.0 equiv *L*-prolinol (Figure 4a). However, the fluorescence enhancement was much smaller for the reaction of (*R*)-**3** with *D*-prolinol under the same conditions (Figure 4b-d). At 6.0 equiv prolinol, the enantioselective fluorescence enhancement ratio [*ef* = (I_L-I_0)/(I_D-I_0)] was found to be 4.5. The fluorescence quantum yield of (*R*)-**3** was found to be <0.01% which increased to 2.40% upon reaction with *L*-prolinol (2 equiv). However, the quantum yield of the reaction of (*R*)-**3** with *D*-prolinol is still <0.01%.

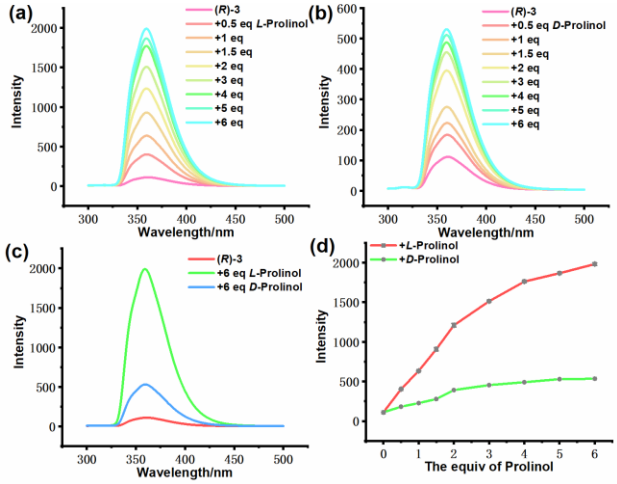

Figure 4. Fluorescence spectra of (*R*)-**3** (2.0×10^{-5} M) with (a) *L*-prolinol, (b) *D*-prolinol, (c) *L*- and *D*-prolinol (6 equiv). (d) Fluorescence intensity at 360 nm versus the equivalent of *L*- and *D*-prolinol. (Solvent: *i*-PrOH. Error bars from three independent experiments. λ_{exc} = 285 nm. Slit: 5/5 nm)

We investigated the fluorescence response of (*S*)-**3**, the enantiomer of (*R*)-**3**, toward *L*- and *D*-prolinol under the same conditions as the use of (*R*)-**3**. As shown in Figure S4 in SI, (*S*)-**3** exhibited greater fluorescence enhancement with *D*-prolinol than with *L*-prolinol. That is, there is a mirror image relation between the fluorescence responses of (*R*)-**3** and (*S*)-**3** toward the enantiomers of prolinol, which confirms the inherent chiral recognition process.

The fluorescence responses of (*R*)- and (*S*)-**3** toward prolinol of various enantiomeric compositions were examined (see Figure S5 in SI). We plotted the fluorescence intensity at λ = 360 nm versus the enantiomeric excess (*ee*) of prolinol in Figure 5. Using this plot, the enantiomeric composition of prolinol can be determined by using the fluorescent probe (*R*)- or (*S*)-**3** at the given concentration. As shown in Figure S6 in SI, the limit of detection (LOD) for *L*-prolinol by using (*R*)-**3** was determined to be 5.30×10^{-8} M.

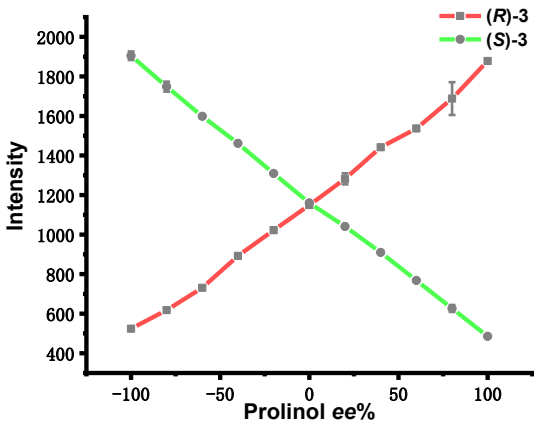

Figure 5. Fluorescence intensity of (*R*)- and (*S*)-**3** (2.0×10^{-5} M) at 360 nm versus prolinol *ee* % [*ee* = (*L*-*D*)/(*L*+*D*)] (4 equiv) (Solvent: *i*-PrOH. Error bars from three independent experiments. λ_{exc} = 285 nm. Slit: 5/5 nm)

We also investigated the fluorescence responses of (*R*)-**3** toward *L*-prolinol (4.0 equiv) in the presence of other amino alcohols (2.0 equiv). As shown by Figure S7 in SI, no significant interference on the fluorescence measurement was observed except with 2-aminocyclohexanol.

In order to understand the observed highly enantioselective fluorescent response, we conducted NMR spectroscopic studies on the reaction of (*R*)-**3** with *L*- and *D*-prolinol. (*R*)-**3** (50.0 mM) was dissolved in CD_3OD, and *L*- and *D*-prolinol (100.0 mM) were dissolved in CD_3OD. An aliquot of the above (*R*)-**3** solution (50 μL) was added to each NMR tube together with varying equivalents of prolinol. Then, CD_3OD was added to reach a volume of 500 μL and the concentration of (*R*)-**3** in each NMR tube was 5.0 mM. After each reaction mixture was allowed to stand at 30 °C for 3 h, their ^{1}H NMR spectra were obtained at room temperature (Figure 6 and Figure S8 in SI). As shown in Figure 6, compound (*R*)-**3** in CD_3OD before addition of prolinol gave two small signals at δ 5.10 and 5.17. These can be attributed to the formation of diastereomeric hemiacetal compounds from the nucleophilic addition of methanol to the aldehyde group of (*R*)-**3**. When (*R*)-**3** was treated with excess amount (> 2 equiv) of *L*- or *D*-prolinol, the aldehyde signal at δ 9.64 disappeared as shown in Figure 6 and Figure S8, indicating the complete conversion of (*R*)-**3**.

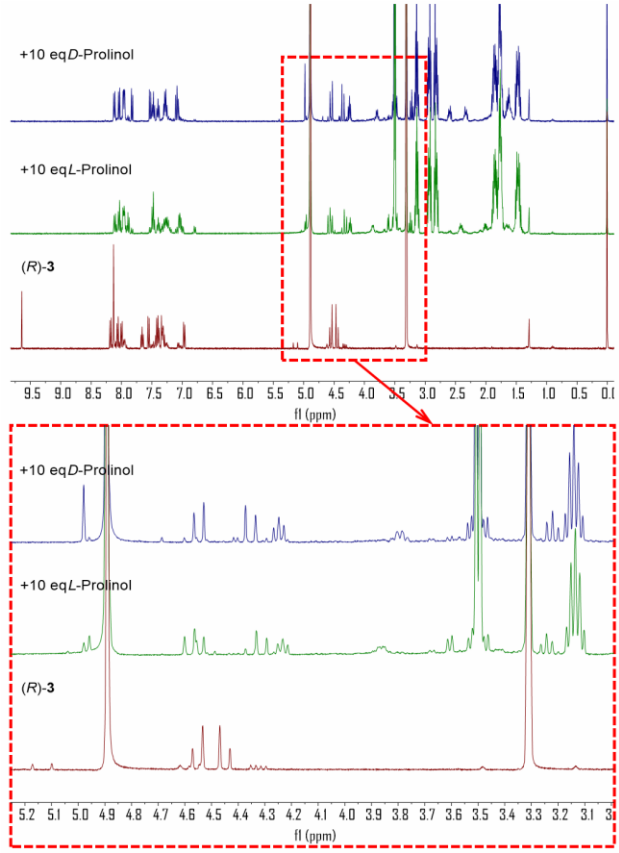

Figure 6. ^{1}H NMR (400 MHz) spectra for the reaction of (*R*)-**3** (5.0 mM) with 10 equiv of *L*-prolinol and *D*-prolinol in CD_3OD. (Reaction time: 3 h.)

Figure 6 shows that the reaction of (*R*)-**3** with excess *D*-prolinol probably gave a single product with well-resolved signals. We thus conducted detailed 1D and 2D ^{1}H and ^{13}C NMR spectroscopic analyses on the product formed from the reaction of (*R*)-**3** with 4.0 equiv *D*-prolinol (see Figure S9 in SI). On the basis of this study, the structure of the product is identified as **17**$_{DS}$. The singlet at δ 4.98 in Figure 6 (with 10 equiv *D*-prolinol) is assigned to H_a on the oxazolidine group of **17**$_{DS}$. The COSY spectrum (see Figure S9a in SI) allows the assignment of H_b [δ 3.78 (m)], H_c and $H_{c'}$ [δ 3.22 and 4.25]. As shown in the zoomed plot of Figure 6 (with 10 equiv *D*-prolinol), both the signals at δ 3.22 and 4.25 are triplet-like because the coupling constants between H_c and $H_{c'}$, H_b and H_c, and H_b and $H_{c'}$ are close to each other. However, it is found that the peak separation Δ (Δ = the peak of the highest frequency – the peak of the lowest frequency) of H_c is 17.0 Hz which is significantly higher than the Δ of $H_{c'}$ (15.3 Hz). This indicates that the coupling of H_b with the *trans* proton H_c is greater than the coupling of H_b with the *cis* proton $H_{c'}$. This is consistent with the relative coupling constants estimated according to the Karplus plot on the basis of the DFT calculated dihedral angle of *trans* H_b-C_b-C_c-H_c (151.8°) versus that of *cis* H_b-C_b-C_c-$H_{c'}$ (27.9°) in **17**$_{DS}$. A NOE effect is observed between H_a and H_c in the NOESY spectrum (see Figure S9d in SI) which allows us to assign a *S* configuration for C_a of compound **17**$_{DS}$. The cross peaks between H_a and C_b (δ 64.11), C_c (δ 72.55) and C_d (δ 53.39) respectively are observed in the 2D ^{1}H-^{13}C HMBC spectrum which supports the bicyclic oxazolidine structure of **17**$_{DS}$ (See Figure S9c in SI). The two diastereotopic proton signals of H_x and $H_{x'}$ in **17**$_{DS}$ were observed at δ 4.53 (d, J = 14.8 Hz) and 4.37 (d, J = 14.9 Hz).

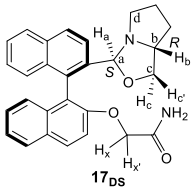

17$_{DS}$

Unlike the reaction of (*R*)-**3** with *D*-prolinol which generates one single product, formation of two products were observed from the reaction of (*R*)-**3** with *L*-prolinol which gave two singlets at δ 4.93 and 4.95 (ratio: 1:0.65). It is proposed that the reaction of (*R*)-**3** with *L*-prolinol might have generated a mixture of both diastereomers **17**$_{LR}$ and **17**$_{LS}$ (Scheme 2). In this mixture, the H_x and $H_{x'}$ signals of these two compounds are partially overlapping in which the signals at δ 4.60 and 4.29 show significant NOE effect with the aromatic signals at δ 7.48 (see Figure S11 in SI).

Scheme 2. Reaction of (*R*)-**3** with *L*-prolinol

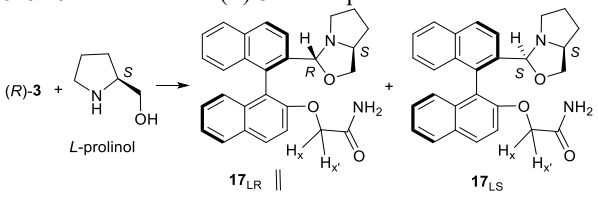

L-prolinol

17$_{LR}$ ‖ **17**$_{LS}$

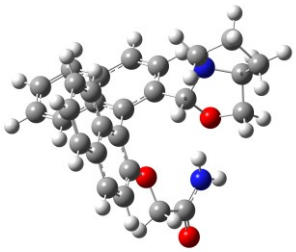

We have conducted TOF mass spectroscopic analysis (ESI) for the products **17** formed from the reaction of (*R*)-**3** with 2.0 equiv *L*- and *D*-prolinol (see Figure S12 in SI). A peak at m/z 439.2017 or 439.2015 (calcd for M+H: 439.2022) in these spectra can be assigned to the molecular ion of **17**. Although we were not able to isolate and purify these products, the NMR and mass spectroscopic analyses have established their structures.

We have conducted DFT calculation on the diastereomers of **17** containing a (*R*)-binaphthyl unit (See Figure S13-S16 in SI). All the quantum chemical calculations are performed with the Gaussian 09 program package and results are analyzed with the Gaussview 6.0 molecular visualization program. Total of four diastereomers are generated which are optimized at the B3LYP, 6-31G(d,p) level in methanol and the ground state energies are calculated. Then, the frequencies of the optimized structure were calculated at B3LYP, 6-31G(d,p), and the number of imaginary frequencies of the four diastereomers with optimized structure are all zero, leading to true minima. It is found that among the four stereoisomers, **17**$_{LR}$ is the most stable one which is formed from the reaction of (*R*)-**3** with *L*-prolinol though the energy difference between **17**$_{LR}$ and **17**$_{LS}$ is small. The energy-minimized molecular modelling structure of **17**$_{LR}$ is given in Scheme 2. The structure of **17**$_{LR}$ shows that the distance between the oxygen atom of the oxazolidine ring and one of the amide hydrogen atoms is 2.0 Å, and the angle O···H-N is 162°. This suggests a possible intramolecular hydrogen bond in **17**$_{LR}$ which could restrict the relative rotation of the binaphthyl unit and contribute to the enhanced fluorescence. The energy difference between the other two diastereomers **17**$_{DS}$ and **17**$_{DR}$ (unobserved) is much greater which leads to the formation of **17**$_{DS}$ as the only product from the reaction of (*R*)-**3** with D-prolinol. Figure 7 lists the calculated relative energies of the four diastereomers formed from the reactions of (*R*)-**3** with D- and L-prolinol.

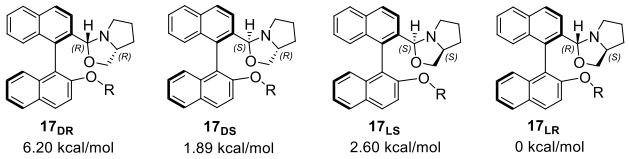

17$_{DR}$ 6.20 kcal/mol | **17**$_{DS}$ 1.89 kcal/mol | **17**$_{LS}$ 2.60 kcal/mol | **17**$_{LR}$ 0 kcal/mol

Figure 7. The DFT calculated relative energies of the four diastereomers **17**$_{DR}$, **17**$_{DS}$, **17**$_{LS}$ and **17**$_{LR}$ (R = CH_2CONH_2) by setting the energy of **17**$_{LR}$ to 0 kcal/mol.

The chemical shift differences between the two diastereotopic protons H_x and $H_{x'}$ in the ^{1}H NMR spectra of (*R*)-**3** are compared with those of **17**$_{DS}$ and **17**$_{LR}$/**17**$_{LS}$. The chemical shift difference between H_x and $H_{x'}$ in (*R*)-**3** is 0.07 ppm and those in **17**$_{DS}$ and **17**$_{LR}$/**17**$_{LS}$ are 0.16 and 0.31 ppm respectively. The much smaller difference in (*R*)-**3** indicates a free rotation of its acetamide group which could minimize the difference in the chemical environment of the two diastereotopic protons. Whereas, the greatly increased difference between the two diastereotopic proton signals of H_x and $H_{x'}$ in **17**$_{LR}$/**17**$_{LS}$ suggests hindered rotation of the acetamide groups in **17**$_{LR}$/**17**$_{LS}$ which could generate more different chemical environment for these two protons. This is consistent with possible intramolecular hydrogen bonding interactions between the acetamide unit and the newly formed oxazolidine ring in these compounds as shown in the DFT calculation. The axial chirality of the binaphthyl core contributes to the energy differences of these diastereomers and their different structural rigidity which have led to the observed enantioselective fluorescence enhancement.

In conclusion, we have discovered a highly chemoselective as well as enantioselective fluorescent probe for the recognition of prolinol. Our spectroscopic studies demonstrate that the reaction of an aldehyde group of the probe with prolinol can generate a bicyclic oxazolidine unit which through a possible intramolecular hydrogen bonding interaction with the acetamide unit of the probe could increase the structural rigidity and produce the observed highly selective fluorescent response. This work employs a design strategy to combine a covalent bond forming unit (an aldehyde group) with a hydrogen bond donor or acceptor to restrict the rotation of a biaryl unit upon selective substrate binding to generate fluorescence enhancement in molecular recognition. This strategy should be generally applicable for the development of fluorescent probes for a variety of substrates.

Experimental Section

General Information. Unless otherwise indicated, all reagents were purchased from commercial sources and used without further purification. In the optical spectroscopic studies, all the solvents were HPLC grade purchased from Thermo Fisher (China) CO. Ltd. NMR spectra were obtained on an Agilent 400-MR DD2 spectrometer. High-resolution mass spectra (HRMS) were obtained with a Shimadzu LCMS-IT-TOF (ESI). Fluorescence spectra were obtained using Hitech F-7000 spectrofluorometer at 298 K. Structural assignments were made with additional information from gCOSY, gHSQC, and gHMBC experiments.

Sample preparation for fluorescence measurement. A stock solution (2.0 mM) of (*R*)-**3** in a solvent such as *i*-PrOH was prepared. Stock solutions (4.0 mM) of the amino alcohols in *i*-PrOH were prepared. For optical analysis, solutions of (*R*)-**3** (25 μL each) were added to several test tubes. A solution of an amino alcohol was added to each test tube and the resulting solution was allowed to stand at 30 °C in a constant temperature and humidity

test chamber. After 3 h, the mixture in each test tube was diluted with *i*-PrOH to obtain 2.0 × 10^{-5} M solutions of (*R*)-**3** for fluorescence measurements. Fluorescence spectra were recorded within 1 h of the sample preparation.

Synthesis and Characterization of (*R*)-3. Compound (*R*)-**2** (100 mg, 0.34 mmol) and K_2CO_3 (93 mg, 0.67 mmol, 2 equiv) were mixed in MeCN (20 mL) at room temperature. 2-Bromoacetamide (71 mg, 0.51 mmol, 1.5 equiv) was added and the resulting mixture was heated under reflux in an oil bath for 24 h. Then the mixture was poured into H_2O (30 mL) at room temperature and extracted with ethyl acetate (3 × 30 mL). The organic extracts were washed with water and dried with Na_2SO_4. The solvent was removed under reduced pressure and the residue was purified by flash column chromatography on silica gel (eluted with ethyl acetate/petroleum ether, 3:2) to afford (*R*)-**3** as a light-yellow solid in 83% yield (100 mg). ^{1}H NMR (400 MHz, chloroform-*d*) δ 9.69 (s, 1H), 8.18 (d, *J* = 8.7 Hz, 1H), 8.08 (dd, *J* = 17.3, 8.8 Hz, 2H), 7.99 (d, *J* = 8.3 Hz, 1H), 7.95 (d, *J* = 8.2 Hz, 1H), 7.66 – 7.60 (m, 1H), 7.46 – 7.40 (m, 1H), 7.40 – 7.28 (m, 4H), 7.08 (d, *J* = 8.5 Hz, 1H), 5.37 (s, 1H), 5.19 (s, 1H), 4.46 (q, *J* = 14.9 Hz, 2H). ^{13}C{^{1}H} NMR (101 MHz, chloroform-*d*) δ 192.5, 170.5, 152.8, 140.8, 136.4, 134.4, 132.5, 132.4, 131.4, 129.5, 129.3, 129.1, 128.7, 128.4, 127.9, 127.5, 126.8, 125.3, 125.0, 122.5, 118.4, 113.7, 68.0. HRMS (ESI-TOF) m/z: [M + Na]$^+$ Calcd for $C_{23}H_{17}NO_3Na$ 378.1106; Found 378.1104. $[\alpha]_D^{25}$ = +11.0 (c = 1.0, $CHCl_3$).

Synthesis and Characterization of (*S*)-3. (*S*)-**3** was prepared in the same way as (*R*)-**3** in 80% yield (97 mg) by starting with (*S*)-**2**. ^{1}H NMR (400 MHz, chloroform-*d*) δ 9.69 (s, 1H), 8.18 (d, *J* = 7.9 Hz, 1H), 8.08 (dd, *J* = 17.1, 8.8 Hz, 2H), 7.99 (d, *J* = 8.2 Hz, 1H), 7.95 (d, *J* = 8.2 Hz, 1H), 7.63 (t, *J* = 7.4 Hz, 1H), 7.46 – 7.40 (m, 1H), 7.40 – 7.28 (m, 4H), 7.08 (d, *J* = 8.5 Hz, 1H), 5.37 (s, 1H), 5.04 (s, 1H), 4.47 (q, *J* = 16.2, 15.5 Hz, 2H). ^{13}C{^{1}H} NMR (101 MHz, chloroform-*d*) δ 192.6, 170.2, 152.9, 140.8, 136.5, 134.5, 132.6, 132.5, 131.5, 129.6, 129.4, 129.2, 128.7, 128.4, 128.0, 127.6, 126.9, 125.4, 125.1, 122.6, 118.5, 113.7, 68.1. HRMS (ESI-TOF) m/z: [M + Na]$^+$ Calcd for $C_{23}H_{17}NO_3Na$ 378.1106; Found 378.1098. $[\alpha]_D^{25}$ = -10.5 (c = 1.0, $CHCl_3$).

Acknowledgement: This work was financially supported by the National Natural Science Foundation of China (22171195) and Sichuan Science and Technology Program (2021YJ0398). LP thanks the partial support of the US National Science Foundation (CHE-1855443 and CHE-2153466). We also thank Jing Li from the Comprehensive Training Platform of Specialized Laboratory in College of Chemistry at Sichuan University for sample analysis.

Data Availability Statement

The data underlying this study are available in the published article and its Supporting Information .

Supplementary Information Available: Additional spectroscopic data and molecular modeling information are provided.

References

1. Reviews on enantioselective fluorescent recognition of chiral organic compounds: a) L. Pu. Fluorescence of Organic Molecules in Chiral Recognition. *Chem. Rev.* **2004**, *104*, 1687. b) D. Leung, S. O. Kang, E. V. Anslyn. Rapid determination of enantiomeric excess: a focus on optical approaches. *Chem. Soc. Rev*. **2012**, *41*, 448. c) A. Accetta, R. Corradini, R. Marchelli. Enantioselective Sensing by Luminescence. *Top. Curr. Chem*. **2011**, *300*, 175. d) X. Zhang, J. Yin, J. Yoon. Recent Advances in Development of Chiral Fluorescent and Colorimetric Sensors. *Chem. Rev*. **2014**, *114*, 4918. e) B. T. Herrera, S. L. Pilicer, E. V. Anslyn, L. A. Joyce, C. Wolf. Optical Analysis of Reaction Yield and Enantiomeric Excess: A New Paradigm Ready for Prime Time. *J. Am. Chem. Soc*. **2018**, *140*, 10385.
2. Reviews on the synthetic applications of chiral amino alcohols: (a) Ager, D**.** J.; Prakash, I**.;** Schaad, D**.** R**.** 1,2-amino alcohols and their heterocyclic derivatives as chiral auxiliaries in asymmetric synthesis. *Chem. Rev*. **1996**, *96*, 835-875. (b) France, S.; Guerin, D. J.; Miller, S. J.; Lectka, T. Nucleophilic chiral amines as catalysts in asymmetric synthesis. *Chem. Rev*. **2003**, *103*, 2985-3012. (c) Fache, F.; Schulz, E.; M. Tommasino, M. L.; Lemaire, M. Nitrogen-containing ligands for asymmetric homogeneous and heterogeneous catalysis. *Chem. Rev*. **2000**, *100*, 2159-2231. (d) Nakano, H.; Owolabi, I. A.; Chennapuram, M.; Okuyama, Y.; Kwon, E.; Seki, C.; Tokiwa, M.; Takeshita, M. *β*-Amino Alcohol Organocatalysts for Asymmetric Additions. *Heterocycles* **2018**, *97*, 647-667. (e) Xu, X**.** J**.**; Wei, H**.;** Feng, H**.** D**.** Synthesis of functionalized oxazolidines by multicomponent reactions of 1,2-amino alcohols (microreview). *Chem. Heterocyclic Compounds* **2020**, *56*, 464-466. (f) Della Sala, G.; Russo, A.; Lattanzi, A. Noncovalent Bifunctional Organocatalysis Mediated by β-Amino Alcohols. *Current Org. Chem*. **2011**, *15*, 2147-2183. (g) Vicario, J. L.; Badia, D.; Carrillo, L.; Reyes, E.; Etxebarria, J. alpha-Amino acids, beta-amino alcohols and related compounds as chiral auxiliaries, Ligands and catalysts in the asymmetric aldol reaction. *Curr. Org. Chem*. **2005**, *9*, 219-235. (h) Zheng, X.; Wang, Y. M. Proline-Catalyzed Asymmetric Reactions. *Prog. Chem.* **2008**, *20*, 1675-1686. (i) Donohoe, T. J.; Callens, C. K. A.; Flores, A.; Lacy, A. R.; Rathi, A. H. Recent Developments in Methodology for the Direct Oxyamination of Olefins. *Chem. Eur. J*. **2011**, *17*, 58-76. (j) Mulahmetovic, E.; Hargaden, G. C. Synthetic Routes to oxazolines. *Mini-Reviews in Org. Chem*. **2019**, *16*, 507-526.
3. Selected references for enantioselective fluorescent recognition of amino alcohols: (a) V. J. Pugh, Q. -H. Hu, L. Pu. The First Dendrimer-Based Enantioselective Fluorescent Sensor for the Recognition of Chiral Amino Alcohols. *Angew. Chem. Int. Ed*. **2000**, *39*, 3638. (b) S. Liu, J. P. C. Pestano, C. Wolf. Enantioselective Fluorescence Sensing of Chiral α-Amino Alcohols. *J. Org. Chem*. **2008**, *73*, 4267. (c) M. M. Wanderley, C. Wang, C. D. Wu, W. B. Lin. A Chiral Porous Metal–Organic Framework for Highly Sensitive and Enantioselective Fluorescence Sensing of Amino Alcohols. *J. Am. Chem. Soc.* **2012**, *134*, 9050. (d) E. G. Shcherbakova, T. Minami, V. Brega, T. D. James, P. Anzenbacher. Determination of Enantiomeric Excess in Amine Derivatives with Molecular Self-Assemblies. *Angew. Chem. Int. Ed.* **2015**, *54*, 7130. (e) P. F. Cai, D. T. Wu, X. Y. Zhao, Y. J. Pan. Fluorescence recognition of chiral amino alcohols by using a novel ionic liquid sensor. *Analyst* **2017**, *142*, 2961. (f) Y. X. Han, W. J. Lv, H. L. Chen, H. Li, J. Chen, Z. Li, H. D. Qiu. Chiral Fluorescent Silicon Nanoparticles for Aminopropanol Enantiomer: Fluorescence Discrimination and Mechanism Identification. *Anal. Chem.* **2020**, *92*, 3949. (g) Y. Sasaki, S. Kojima, V. Hamedpour, R. Kubota, S. Takizawa, I. Yoshikawa, H. Houjou, Y. Kubo, T. Minami. Accurate chiral pattern recognition for amines from just a single chemosensor. *Chem. Sci.* **2020**, *11*, 3790. (h) K. Guo, P. Wang, W. L. Tan, Y. Li, X. W. Gao, Q. Wang, L. Pu. Structure of a Dimeric BINOL-Imine-Zn(II) Complex and Its Role in Enantioselective Fluorescent Recognition. *Inorg. Chem.* **2020**, *59*, 17992. (i) E. G. Shcherbakova, T. D. James, P. Anzenbacher. High-throughput assay for determining enantiomeric excess of chiral diols, amino alcohols, and amines and for direct asymmetric reaction screening. *Nat Protoc* **2020**, *15*, 2203. (j) C. Yuan, S. G. Fu, K. W. Yang, B. Hou, Y. Liu, W. Y. Jiang, Y. Cui. Crystalline C-C and C═C Bond-Linked Chiral Covalent Organic Frameworks. *J. Am. Chem. Soc.* **2021**, *143*, 369. (k) J. J. Jiao, J. Q. Dong, Y. G. Li, Y. Cui. Fine-Tuning of Chiral Microenvironments within Triple-Stranded Helicates for Enhanced Enantioselectivity. *Angew. Chem. Int. Ed.* **2021**, *60*, 16568.
4. In the absence of Zn^{2+}: Hu, L. L.; Yu, S. S.; Wang, Y. C.; Yu, X .Q.; Pu, L. Enhanced Fluorescence of 3,3′-Diformyl BINOL by Functional Secondary Amines. *Org. Lett.* **2017**, *19*, 3779-3782.
5. In the presence of Zn^{2+}, (*R*)-**1** shows enantioselective fluorescent response toward certain functional chiral amines: Huang, Z.; Yu, S. S.; Yu, X. Q.; Pu. L. Zn(II) Promoted Dramatic Enhancement in the Enantioselective Fluorescent Recognition of Functional Chiral Amines by a Chiral Aldehyde. *Chem. Sci.* **2014**, *5*, 3457-3462.
6. Tian, J.; Wang, Y.L.; Chen, Y.; Zhao, F.; Jiang, Y. X.; Yu, S. S.; Yu, X. Q.; Pu, L. Chemoselective and enantioselective fluorescent recognition of glutamic and aspartic acids. *Chem. Commun.* **2020**, *56*,

15012-15015.
7. Tian, J.; Lu, K.; Wang, Y. L.; Chen, Y.; Huo, B. Y.; Jiang, Y. X.; Yu, S. S.; Yu, X. Q.; Pu, L. A metal-free fluorescent probe for selective detection of histidine. *Tetrahedron* **2021**, *95*, 132366.
8. Selected examples: (a) Pasuparthy, S. D.; Maiti, B. Enantioselective Organocatalytic Michael Addition Reactions Catalyzed by Proline/ Prolinol/ Supported Proline based Organocatalysts: An Overview. *Chemistry Select* **2022**, *7*, e202104261. (b) Li Petri, G.; Raimondi, M. V.; Spano, V.; Holl, R.; Barraja, P.; Montalbano, A. Pyrrolidine in Drug Discovery: A Versatile Scaffold for Novel Biologically Active Compounds. *Toc. Curr. Chem*. **2021**, *379*, 34.
9. Vermeersch, K. A.; Wang, L.; McDonald, J. F.; Styczynski, M. P. Distinct metabolic responses of an ovarian cancer stem cell line. *BMC Systems Biology* **2014**, *8*, 134.